AD-A214 451

Short-rise-time microwave pulse propagation through dispersive biological media

Richard A. Albanese, John Penn, and Richard Medina

Radiation Sciences Division, United States Air Force School of Aerospace Medicine, Brooks Air Force Base, San Antonio, Texas 78235-5301

Numerical research is reported on the propagation of short microwave pulses into living, biological materials. These materials are dispersive, and data on the dielectric constant and conductivity for these materials follow a Debye model. A Fourier-series calculation is presented that predicts the occurrence of Brillouin precursors when the incident pulses have sufficiently short rise times. These transients are attenuated with increasing propagation distance but are attenuated more slowly than the carrier frequency of the pulse, which is attenuated exponentially with distance. An analysis of the numerical error resulting from truncation of the Fourier series is given. Upper-bound estimates of truncation error show good series convergence.

1. INTRODUCTION

Microwave engineers are currently developing radiating devices that generate short, high-energy pulses.[1-3] As a result it is a matter of considerable medical interest to determine precisely the dynamical evolution of these pulses as they progress through living tissue, in order to obtain an assessment of possible health effects in workers exposed to these signals.

In this paper we describe some recent numerical research on the dynamical evolution of short-rise-time microwave pulses that are transmitted into tissue. Since tissue is composed largely of water, we have directed considerable attention to the study of pulse propagation through this material. The frequency dependences of both the relative dielectric constant, ϵ_r, and the conductance, σ, of pure water are shown in Fig. 1. These curves have been computed from Eqs. (1.1) which were provided to us by Grant[4]:

$$\epsilon_r = 5.5 + 72.7/[1 + (\omega T)^2],$$
$$\sigma = 10^{-5} + 72.7\omega^2\epsilon_0 T/[1 + (\omega T)^2]. \quad (1.1)$$

These equations were determined by fitting experimental data to a Debye model medium, and they apply for frequencies ω from dc to 10^{11} Hz at a temperature of 25°C. Here ϵ_0 is the permittivity of free space, $T = 8.1 \times 10^{-12}$ sec is the relaxation time, and $\omega = 2\pi f$, in which f is the frequency in hertz. For frequencies $>10^{11}$ Hz we have used data that were calculated from values for the index of refraction and the absorption coefficient provided in Fig. 7.9 of Ref. 5.

2. INCIDENT WAVEFORMS STUDIED

We have studied incident pulses that are formed by trapezoidal modulation of a sinusoidal field of fixed angular frequency ω. Our approach is to treat individual pulses as members of a pulse train, so that the analysis is amenable to a Fourier-series analysis. A typical trapezoidally modulated incident signal (in vacuum) is shown in Fig. 2 and is given by

$$
\begin{aligned}
E(z, t) &= (1/a)(t - z/c)\sin[\omega(t - z/c)] && \text{for } 0 < (t - z)/c < a \\
&= \sin[\omega(t - z/c)] && \text{for } a < (t - z/c) < (\tau - a) \\
&= \{1 - (1/a)[t - z/c - (\tau - a)]\}\sin[\omega(t - z/c)] && \text{for } (\tau - a) < (t - z/c) < \tau \\
&= 0 && \text{for } \tau < (t - z/c) < L, \quad (2.1)
\end{aligned}
$$

in which c is the speed of light in vacuum. The parameter a is the rise-time parameter for the pulse envelope and is simply the time that it takes for the modulation to rise to its maximum value. We have generally assumed that the maximum amplitude of our incident signals is 1 V/m. The signal described in Eq. (2.1) is repeated with a period L, so that the Fourier series of the pulse train is

$$E(z, t) = \sum_{n=1}^{\infty} (A_n{}^2 + B_n{}^2)^{1/2}\sin[\lambda_n(t - z/c) + \phi_n], \quad (2.2)$$

for which

$$
\begin{aligned}
aLA_n &= [\sin(\omega + \lambda_n)a + \sin(\omega + \lambda_n)(\tau - a) \\
&\quad - \sin(\omega + \lambda_n)\tau]/(\omega + \lambda_n)^2 + [\sin(\omega - \lambda_n)a \\
&\quad + \sin(\omega - \lambda_n)(\tau - a) - \sin(\omega - \lambda_n)\tau]/(\omega - \lambda_n)^2,
\end{aligned}
$$

$$
\begin{aligned}
aLB_n &= [1 - \cos(\omega + \lambda_n)a + \cos(\omega + \lambda_n)\tau \\
&\quad - \cos(\omega + \lambda_n)(\tau - a)]/(\omega + \lambda_n)^2 + [-1 + \cos(\omega - \lambda_n)a \\
&\quad - \cos(\omega - \lambda_n)\tau + \cos(\omega - \lambda_n)(\tau - a)]/(\omega - \lambda_n)^2,
\end{aligned}
$$

where $\lambda_n = 2\pi n/L$ and $\tan \phi_n = A_n/B_n$.

As the rise-time parameter a approaches zero, we find, by using L'Hôpital's rule, that

$$\lim_{a \to 0} A_n = 2\omega(1 - \cos \lambda_n\tau)L(\omega^2 - \lambda_n{}^2),$$

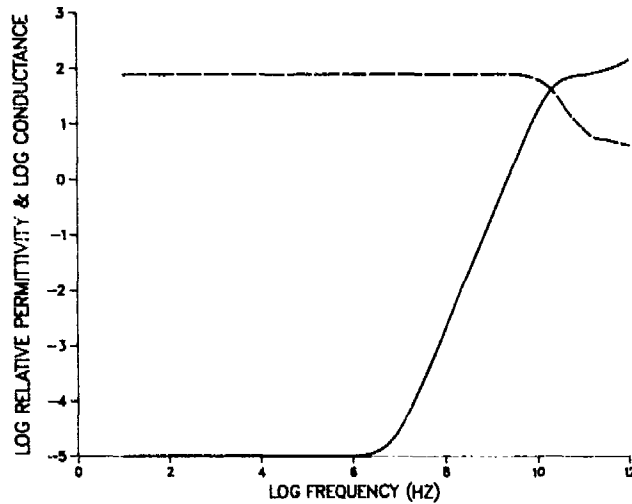$$\lim_{a \to 0} B_n = -2\omega \sin \lambda_n\tau/L(\omega^2 - \lambda_n{}^2).$$

89 11 16 110

Fig. 1. Relative permittivity or dielectric constant (dashed line) and conductance (in reciprocal ohms per meter), shown as functions of frequency. Logarithmic scales are used.
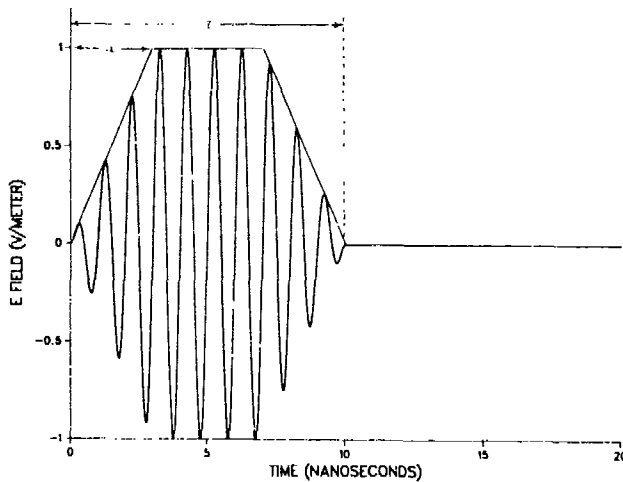

Fig. 2. Example trapezoidal pulse. The trapezoidal envelope can be modified to achieve the extremes of square-wave or triangular-wave modulation.

Therefore, a square-wave-modulated sinusoidal pulse train has the Fourier series

$$E(z, t) = \sum_{n=1}^{\infty} C_n \sin[\lambda_n(t - z/c) + \phi_n], \qquad (2.3)$$

in which

$$C_n = -4\omega \sin(\lambda_n\tau/2)/L(\omega^2 - \lambda_n^2),$$

$$\phi_n = -\lambda_n\tau/2.$$

The strategy of our analysis is to use these Fourier-series representations of the incident pulse train, to propagate each Fourier component individually into the structure of interest by using Maxwell's equations, and then to sum the individual transmitted sinusoids to reconstruct the propagated response to the pulse train. The pulses in the incident pulse train are assumed to be spaced widely enough apart so that there is no mutual interference of the pulses within the target structure.

3   EQUATIONS FOR TRANSMITTED WAVES

The Fourier series for transmitted pulse trains are now considered for the half-space geometry. The analysis begins with Maxwell's equations, which assume the following form for our problem:

$$\nabla \times \mathbf{E} = -\partial\mathbf{B}/\partial t,$$
$$\nabla \times \mathbf{H} = \mathbf{J} + \partial\mathbf{D}/\partial t,$$
$$\nabla \cdot \mathbf{D} = 0,$$
$$\nabla \cdot \mathbf{H} = 0. \qquad (3.1)$$

Here $\mathbf{B} = \mu_0\mathbf{H}$ because tissue is believed, at this time, to have the magnetic properties of a vacuum. In addition, ρ is taken to be zero.

In order to include the dependence of σ and ϵ on the frequency for a homogeneous, isotropic, locally linear casual medium filling the half-space $z > 0$, we express the conduction current $\mathbf{J}(r, t)$ in the constitutive relation

$$\mathbf{J}(r, t) = \int_0^{\infty} W_J(u)\mathbf{E}(r, t - u)du, \qquad (3.2a)$$

in which $W_J(u)$ is the conduction current impulse response. Also, the displacement vector $\mathbf{D}(r, t)$ is given by the constitutive relation

$$\mathbf{D}(r, t) = \int_0^{\infty} W_D(u)\mathbf{E}(r, t - u)du, \qquad (3.2b)$$

in which $W_D(u)$ is the displacement impulse response.

Applying Maxwell's equations [Eqs. (3.1)] with the above constitutive relations to plane-wave propagation, in the z direction, we seek solutions of the form $\xi = \xi_S(z)\exp(i\lambda t)$ and find, as is well known, that such solutions must obey the Helmholtz equation,

$$\partial^2\xi_s/\partial z^2 + \kappa^2\xi_s = 0, \qquad (3.3)$$

in which

$$\kappa^2 = \lambda^2\mu_0\epsilon - i\lambda\mu_0\sigma. \qquad (3.4)$$

Notice that the permittivity is given here by

$$\epsilon = \text{Re}(\tilde{W}_D) + \text{Im}(\tilde{W}_J)/\omega \qquad (3.5)$$

and the conductivity is given by

$$\sigma = \text{Re}(\tilde{W}_J) - \omega\,\text{Im}(\tilde{W}_D), \qquad (3.6)$$

in which a tilde over a function's symbol indicates the Fourier transform of the function. These relations show that in a dispersive medium such as tissue, in which there can be separate processes underlying the conduction and polarization, ϵ and σ can each relate to both processes.

Representing κ as $\beta - i\alpha$, we obtain the plane-wave phase factor β as

$$\beta = \lambda(\mu_0\epsilon/2)^{1/2}\{1 + [1 + (\sigma/\lambda\epsilon)^2]^{1/2}\}^{1/2} \qquad (3.7)$$

and the amplitude attenuation coefficient α as

$$\alpha = \lambda(\mu_0\epsilon/2)^{1/2}\{-1 + [1 + (\sigma/\lambda\epsilon)^2]^{1/2}\}^{1/2}. \qquad (3.8)$$

The half-space geometry considered here is shown in Fig. 3. In the half-space $z < 0$, the wave factors α_I and β_I relate to the vacuum, so that $\beta_I = \lambda/c$ and $\alpha_I = 0$. In the half-space z
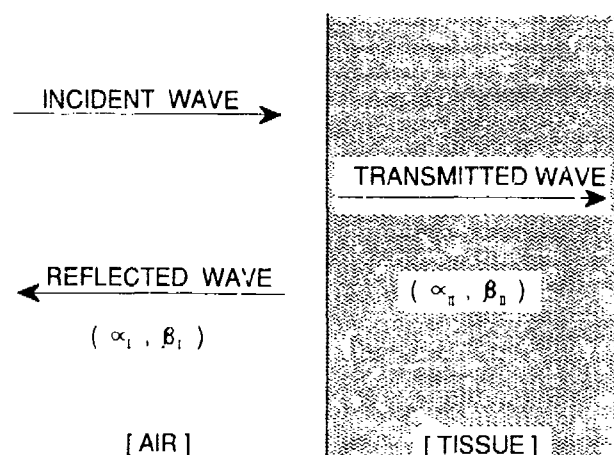
Fig. 3.   Diagram of the half-space geometry studied in this paper.

> 0, the wave factors α_{II} and β_{II} describe the tissue, so that α_{II} and β_{II} depend on $\mu = \mu_0$, $\epsilon = \epsilon(\lambda)$, and $\sigma = \sigma(\lambda)$. Application of the boundary conditions then yields the complex transmitted field $\xi_{trans}(z, t)$ in the form

$$\xi_{trans}(z, t) = 2E_i \frac{(\beta_1 - i\alpha_1)}{(\beta_1 - i\alpha_1) + (\beta_{II} - i\alpha_{II})}$$

$$\times \exp[-\alpha_{II}z + i(\lambda t - \beta_{II}z)], \quad (3.9)$$

in response to an incident wave $E_i \exp[i\lambda(t - z)/c)]$.

After taking the imaginary part of $\xi_{trans}(z, t)$ we find that, for a continuous incident wave of the form $E_{inc}(z, t) = E_i \sin[\lambda(t - z/c)]$, the transmitted wave at depth z in the half-space $z > 0$ is given by

$$E_{trans} = \frac{2E_i \exp(-\alpha_{II}z)\sin(\lambda t - \beta_{II}z + \theta)}{[(1 + \beta_{II}c/\lambda)^2 + (\alpha_{II}c/\lambda)^2]^{1/2}}, \quad (3.10)$$

in which the phase angle θ is specified by

$$\tan \theta = \alpha_{II}/[(\lambda/c) + \beta_{II}]. \quad (3.11)$$

Therefore, if a pulse train such as that given by Eq. (2.2) is incident upon the half-space, the transmitted wave is given by the summation

$$E_{trans}(z, t)$$

$$= 2 \sum_{n=1}^{\infty} \frac{(A_n^2 + B_n^2)^{1/2}\exp(-\alpha_{II,n}z)\sin(\lambda t - \beta_{II,n}z + \phi_n + \theta_n)}{[(1 + \beta_{II,n}c/\lambda)^2 + (\alpha_{II,n}c/\lambda)^2]^{1/2}}$$

$$(3.12)$$

In this expression the quantities $\alpha_{II,n}$ and $\beta_{II,n}$ are simply α_{II} and β_{II} calculated at λ_n. Similarly, θ_n is θ, as given above, calculated by using $\alpha_{II,n}$ and $\beta_{II,n}$. For a square-wave-modulated sinusoidal incident wave, the quantity $(A_n^2 + B_n^2)^{1/2}$ appearing in Eq. (2.2) is replaced by C_n.

4. RESULTS

Sommerfeld,[6] Brillouin,[7] and Oughstun and Sherman[8,9] used asymptotic analyses to show that a Heaviside unit-step-function-modulated sinusoidal field produces fundamental transient fields, called precursors, in a medium exhibiting anomalous dispersion. Our analysis is concerned with water and other similar media that do not exhibit anomalous dispersion in the frequency regime relevant to microwave pulses. Inspection of Eq. (3.12) shows that it is likely that significant pulse deformation or blurring will occur on propagation into the medium, but it is not evident that any recognizable transients will result.
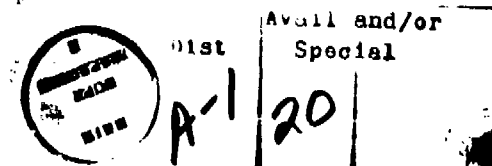
In fact, from computations of the transmitted propagated field with Eq. (3.12) we have noticed a well-formed transient field that appears similar to the Brillouin precursor observed in media with anomalous dispersion. On the other hand, thus far in our numerical research we have observed no evidence of the Sommerfeld precursor when we use dielectric constant and conductivity data as shown in Fig. 1. In part, this is because the Brillouin precursor is a low-frequency transient field and so is excited more readily by an input microwave field, whereas the Sommerfeld precursor is a high-frequency transient field and is not excited so readily by such a low-frequency input field.

Figure 4 shows examples of transmitted waves at increasing propagation distances in the half-space $z > 0$ when the incident wave is a square-wave-modulated 1-GHz sinusoid. The transient-field formation is most pronounced at greater propagation depths. The 1-GHz carrier frequency is attenuated exponentially, as is expected, but the peak transient-field amplitude decreases much more slowly. This is shown in Fig. 5, in which the peak of the leading transient is plotted, along with the amplitude of the fundamental frequency, as a function of depth in the half-space. This behavior is in agreement with the asymptotic analysis of Ref. 9, in which it is shown that the peak amplitude in the Brillouin precursor decreases only as $z^{-1/2}$.

In addition, we have found that the transient-field formation is influenced sensitively by the nature of the pulse modulation. Specifically, increasing values of the initial rise-time parameter a in the trapezoidally modulated field results in decreasing amplitudes of the transient fields formed, including a reversal of the polarity of the transient-field peak, depending on the size of a. This is illustrated in Fig. 6, which shows plots of the transmitted signals at 150 cm into a water half-space for increasing values of the rise-time parameter a.

Our numerical calculations for 10-GHz square-wave-modulated signals produce pulse waveform patterns that are strictly analogous to those shown in Fig. 4 for the 1-GHz pulses with the exception of a simple scaling by the penetration distance. For example, Fig. 7 shows a plot of the transient peak amplitude and the amplitude of the fundamental frequency versus the propagation distance, and this is seen to be similar to that depicted in Fig. 5 when the distance axis is scaled linearly.

The numerical results displayed in Figs. 4–7 were obtained by direct numerical calculation, using Eq. (3.12). For each frequency λ_n of the Fourier series we used a value of $\epsilon(\lambda_n)$ and a value of $\sigma(\lambda_n)$ taken from a spline fit of the data in Fig. 1. In the case of the 1-GHz pulse, τ was 10 nsec in duration and L was 20 nsec in duration. In the case of the 10-GHz pulse, τ was 1 nsec and L was 2 nsec. We have found in all our calculations thus far that, when $L \geq 2\tau$, individual pulses in the pulse train do not interact and therefore, when the pulses are adequately spaced, one obtains simply the individual pulse response.
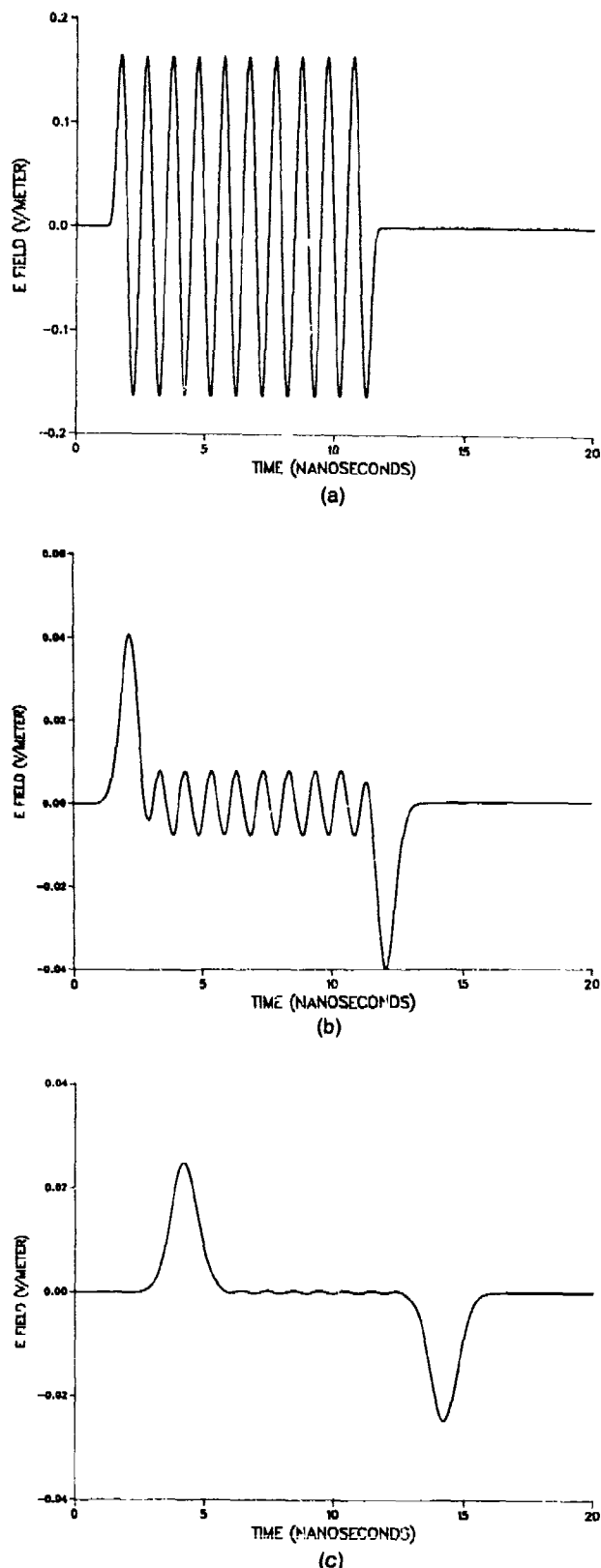
(a)

(b)

Fig. 4. Transmitted wave at depths of (a) 5 cm, (b) 75 cm, and (c) 150 cm in a water half-space when the incident wave is a square-wave-modulated, 1-V/m, 1-GHz sinusoidal field orthogonally incident upon the air–half-space interface.
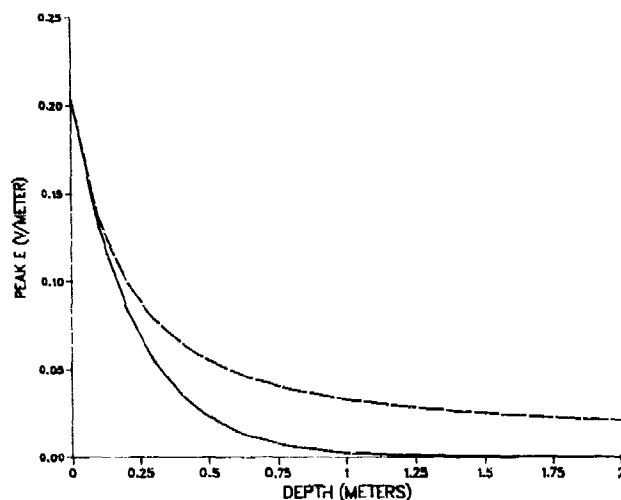

Fig. 5.   Peak of the leading transient (dashed curve) and amplitude of the fundamental frequency (solid-curve), as functions of the propagation depth in the half-space $z > 0$ for the 1-GHz, square-wave-modulated signal.

We have calculated the transmitted wave by using Eq. (3.12) and summing over the coefficients from $n = 1$ to and including $n = 512$. Truncation error, caused by failure to sum terms associated with $n > 512$ can be evaluated directly from Eq. (3.12). For example, for a square-wave-modulated incident wave, the neglected signal $R_{513}(z, t)$ is given by

$$R_{513}(z, t)$$

$$= 2 \sum_{n=513}^{\infty} \frac{C_n \exp(-\alpha_{II,n}z)\sin(\lambda t - \beta_{II,n}z + \phi_n + \theta_n)}{[(1 + \beta_{II,n}c/\lambda)^2 + (\alpha_{II,n}c/\lambda)^2]^{1/2}}. \quad (4.1)$$

Since $\alpha_{II,n}$ and $\beta_{II,n}$ are both always greater than or equal to 0, and since $\exp(-\alpha_{II,n}z)$ and $\sin(u)$ are always less than or equal to 1,

$$R_{513}(z, t) \leqq 2 \sum_{n=513}^{\infty} \frac{4\omega}{L(\lambda_n^2 - \omega^2)} < \frac{8\omega}{L(\lambda_{513}^2 - \omega^2)}$$

$$+ \frac{8\omega}{L} \int_{513}^{\infty} \frac{dn}{(\lambda_n^2 - \omega^2)}. \quad (4.2)$$

It then follows that the neglected signal satisfies the inequality

$$R_{513}(z, t) < \frac{8\omega}{L(\lambda_{513}^2 - \omega^2)} - \frac{2}{\pi} \ln \frac{\lambda_{513} - \omega}{\lambda_{513} + \omega}. \quad (4.3)$$

This last expression demonstrates that the series for the transmitted wave converges for all $z \geqq 0$. For the 1-GHz square-wave-modulated pulse studied in this report, $R_{513}(z, t) < 0.0248$ V/m. Improved estimates of $R_{513}(z, t)$ for $z > 0$ can be calculated by carrying the attenuation term $\exp(-\alpha_{II,n}z)$ in the estimate. By doing this, one finds a progressive decrease in the truncation error with increasing propagation distance. As empirical evidence, when we use
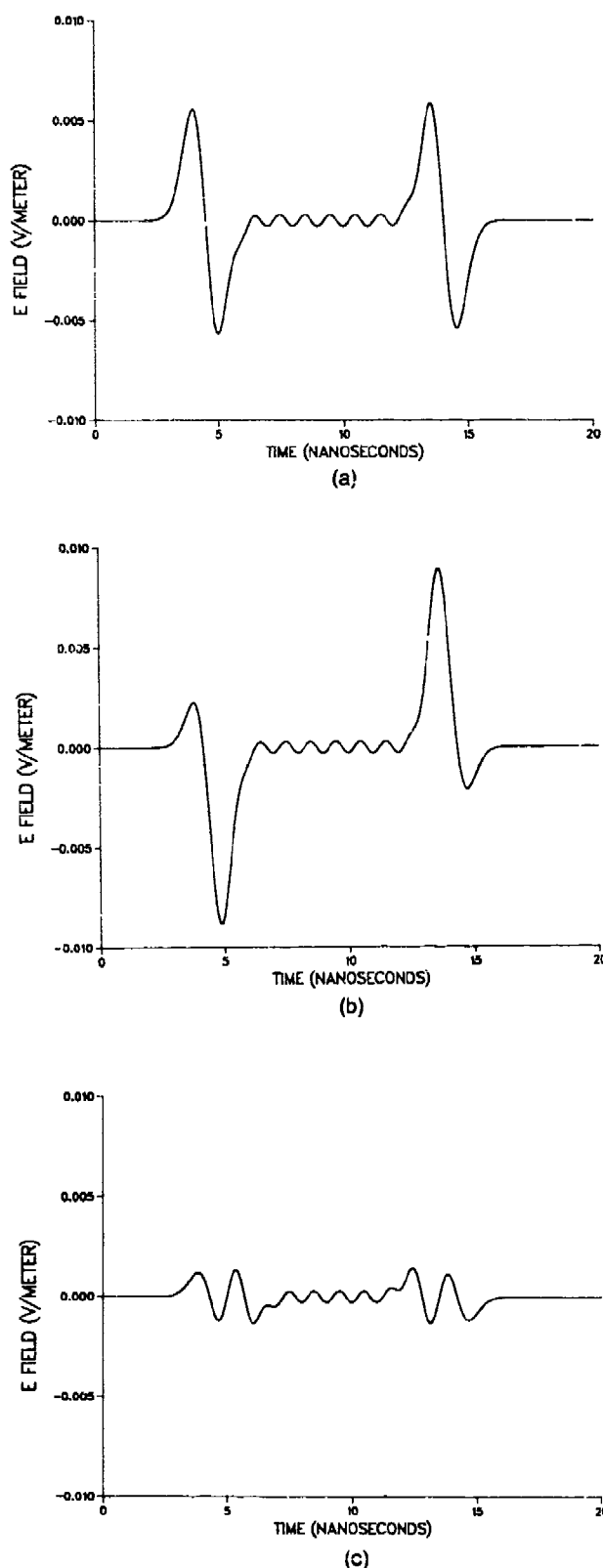
(a)

(b)

(c)

Fig. 6.   Transmitted wave at a depth of 150 cm in a water half-space for an incident wave that is a trapezoidally modulated, 1-V/m, 1-GHz sinusoid. The rise-time parameter a, the time to reach the maximum value of the trapezoidal modulation, is set at (a) $1/(2f)$ sec, (b) $3/(4f)$ sec, and (c) $3/(2f)$ sec.
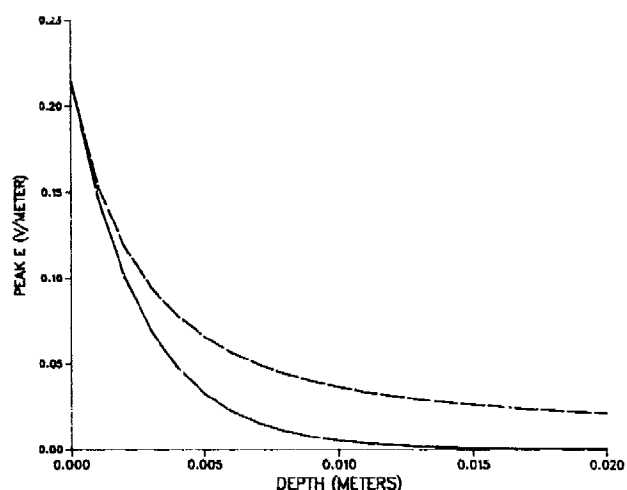

Fig. 7.   Peak of the leading transient (dashed curve) and the amplitude of the fundamental frequency (solid curve), as functions of the propagation depth in the half-space $z > 0$ for the 10-GHz, square-wave-modulated signal.

1000 or more coefficients to calculate transients, we generally note amplitude changes, compared with the 500-coefficient calculation, in only the fourth or fifth decimal place. By comparison, although a similar approach using the fast-Fourier-transform algorithm significantly increases the speed of calculation and seems to work quite well, we have not yet been able to develop an estimate of the error of the calculated transmitted wave because of the finite sampling of the incident signal.

Experiments have been performed at Physics International Company in San Leandro, California, to test the above-described theory of pulse propagation. Pulse propagation in a coaxial test cell and in an open-field tissue-equivalent test structure has followed the numerical predictions closely. This research will be reported fully elsewhere.

5. CONCLUSION

We conclude that a short-rise-time microwave pulse can create a disturbance in tissue at a greater depth than would be expected if one were to use the depth of penetration of the basic carrier frequency ω. This finding should be of interest to those who are studying or otherwise evaluating human exposures to electromagnetic devices that produce such pulses. In addition, from our calculations of square-wave-modulated sinusoidal signals, we have observed a transient field in water that is similar to the second or Brillouin precursors that were described asymptotically by Brillouin[7] and by Oughstun and Sherman.[8,9] Finally, we have observed that, for trapezoidal modulation of the input field, this transient field decreases in amplitude as the time to reach the maximum of the trapezoidal modulation is increased, and an inversion of the transient polarity is produced.

ACKNOWLEDGMENT

REFERENCES

1. J. Benford, D. Price, H. Sze, and D. Bromley, "Interaction of a vircator microwave generator with an enclosing resonant cavity," J. Appl. Phys. **61**, 2098–2100 (1987).
2. H. Sze, J. Benford, W. Woo, and B. Harteneck, "Dynamics of a virtual cathode oscillator driven by a pinched diode," Phys. Fluids **29**, 3873–3880 (1986).
3. J. Benford, H. Sze, T. Young, D. Bromley, and G. Prouix, "Variations on the relativistic magnetron," IEEE Trans. Plasma Sci. **PS-13**, 538–544 (1985).
4. E. H. Grant, King's College, University of London, London, UK (personal communication, 1988). See also E. H. Grant, R. J. Sheppard, and G. P. South, *Dielectric Behaviour of Biological Molecules in Solution* (Clarendon, Oxford, 1978).
5. J. D. Jackson, *Classical Electrodynamics* (Wiley, New York, 1975).
6. A. Sommerfeld, "Über die Fortpflanzung des Lichtes in disperdierenden Medien," Ann. Phys. **44**, 177–202 (1914).
7. L. Brillouin, "Über die Fortpflanzung des Lichtes in disperdierenden Medien," Ann. Phys. **44**, 203–240 (1914).
8. G. C. Sherman and K. E. Oughstun, "Description of pulse dynamics in Lorentz media in terms of energy velocity and attenuation of time-harmonic waves," Phys. Rev. Lett. **47**, 1451–1454 (1981).
9. K. E. Oughstun and G. C. Sherman, "Propagation of electromagnetic pulses in a linear dispersive medium with absorption (the Lorentz medium)," J. Opt. Soc. Am. B **5**, 817–849 (1988).

REPORT DOCUMENTATION PAGE

1a. REPORT SECURITY CLASSIFICATION UNCLASSIFIED		1b. RESTRICTIVE MARKINGS		
2a. SECURITY CLASSIFICATION AUTHORITY		3. DISTRIBUTION/AVAILABILITY OF REPORT Approved for public release; distribution is unlimited.		
2b. DECLASSIFICATION/DOWNGRADING SCHEDULE				
4. PERFORMING ORGANIZATION REPORT NUMBER(S) USAFSAM-JA-88-71		5. MONITORING ORGANIZATION REPORT NUMBER(S) Not Applicable		
6a. NAME OF PERFORMING ORGANIZATION USAF School of Aerospace Medicine	6b. OFFICE SYMBOL *(If applicable)* USAFSAM/RZM	7a. NAME OF MONITORING ORGANIZATION Not Applicable		
6c. ADDRESS *(City, State, and ZIP Code)* Human Systems Division (AFSC) Brooks Air Force Base, TX 78235-5301		7b. ADDRESS *(City, State, and ZIP Code)*		
8a. NAME OF FUNDING/SPONSORING ORGANIZATION	8b. OFFICE SYMBOL *(If applicable)*	9. PROCUREMENT INSTRUMENT IDENTIFICATION NUMBER		
8c. ADDRESS *(City, State, and ZIP Code)*		10. SOURCE OF FUNDING NUMBERS		

	PROGRAM ELEMENT NO.	PROJECT NO.	TASK NO.	WORK UNIT ACCESSION NO.
	62202F	7757	01	2C

11. TITLE *(Include Security Classification)*
Short-rise-time microwave pulse propagation through biological media.

12. PERSONAL AUTHOR(S)
Richard Albanese, John Penn, Richard Medina

13a. TYPE OF REPORT Interim	13b. TIME COVERED FROM 82/1/1 TO 89/1/1	14. DATE OF REPORT *(Year, Month, Day)* 1989 January 9	15. PAGE COUNT 6

16. SUPPLEMENTARY NOTATION

17. COSATI CODES			18. SUBJECT TERMS *(Continue on reverse if necessary and identify by block number)*
FIELD	GROUP	SUB-GROUP	Electromagnetic Pulse
20	15		Electromagnetic Propagation
20	14		

19. ABSTRACT *(Continue on reverse if necessary and identify by block number)*
Numerical research is reported on the propagation of short microwave pulses into living, biological materials. These materials are dispersive, and data on the dielectric constant and conductivity for these materials follow a Debye model. A Fourier-series calculation is presented that predicts the occurrence of Brillouin precursors when the incident pulses have sufficiently short rise times. These transients are attenuated with increasing propagation distance, but are attenuated more slowly than the carrier frequency of the pulse, which is attenuated exponentially with distance. At analysis of the numerical error resulting from truncation of the Fourier series is given. Upperbound estimates of truncation error show good series convergence.

20. DISTRIBUTION/AVAILABILITY OF ABSTRACT ☒ UNCLASSIFIED/UNLIMITED ☐ SAME AS RPT. ☐ DTIC USERS	21. ABSTRACT SECURITY CLASSIFICATION UNCLASSIFIED	
22a. NAME OF RESPONSIBLE INDIVIDUAL Richard A. Albanese, MD.	22b. TELEPHONE *(Include Area Code)* 512-536-3882	22c. OFFICE SYMBOL USAFSAM/RZM

DD Form 1473, JUN 86   *Previous editions are obsolete.*